J. Anat. (2006) **209**, pp93–110

Reconstructing impairment of secretory ameloblast function in porcine teeth by analysis of morphological alterations in dental enamel

Carsten Witzel,[1,5] Uwe Kierdorf,[1] Keith Dobney,[2] Anton Ervynck,[3] Sofie Vanpoucke[4] and Horst Kierdorf[1]

[1]*Department of Biology, University of Hildesheim, Germany*
[2]*Department of Archaeology, University of Durham, UK*
[3]*Flemish Heritage Institute, Brussels, Belgium*
[4]*Department of Archaeology, University of Leuven, Belgium*
[5]*Institute of Anthropology, University of Giessen, Germany*

Abstract

We studied the relationship between the macroscopic appearance of hypoplastic defects in the dental enamel of wild boar and domestic pigs, and microstructural enamel changes, at both the light and the scanning electron microscopic levels. Deviations from normal enamel microstructure were used to reconstruct the functional and related morphological changes of the secretory ameloblasts caused by the action of stress factors during amelogenesis. The deduced reaction pattern of the secretory ameloblasts can be grouped in a sequence of increasingly severe impairments of cell function. The reactions ranged from a slight enhancement of the periodicity of enamel matrix secretion, over a temporary reduction in the amount of secreted enamel matrix, with reduction of the distal portion of the Tomes' process, to either a temporary or a definite cessation of matrix formation. The results demonstrate that analysis of structural changes in dental enamel allows a detailed reconstruction of the reaction of secretory ameloblasts to stress events, enabling an assessment of duration and intensity of these events. Analysing the deviations from normal enamel microstructure provides a deeper insight into the cellular changes underlying the formation of hypoplastic enamel defects than can be achieved by mere inspection of tooth surface characteristics alone.

Key words domestic pig; enamel hypoplasia; enamel microstructure; *Sus scrofa*; teeth; wild boar.

Introduction

Mature dental enamel consists of about 96% inorganic constituents (by weight) and is the most highly mineralized tissue of the mammalian body (Nanci, 2003). Enamel is cell-free, and incapable of repair or remodelling (Boyde, 1989; Hillson, 1996). It is formed by specialized ectodermal cells, the ameloblasts, which differentiate from the cells of the inner dental epithelium. Amelogenesis can be roughly divided into a secretory stage, during which a proteinaceous matrix is secreted that becomes initially mineralized, and a subsequent maturation stage, during which this matrix is enzymatically degraded and resorbed, and further, intense mineral growth takes place (Warshawsky, 1988; Boyde, 1989; Sasaki et al. 1997; Smith, 1998; Nanci, 2003). Because enamel does not repair or remodel, structural aberrations caused by a disturbance of enamel formation leave a permanent record in the tissue. As the microstructural organization of enamel is closely related to the morphology of the secretory ameloblast, alterations of enamel structure can be used to reconstruct the impact of various stress factors on the secretory ameloblasts.

Enamel hypoplasia develops as a consequence of an impairment of enamel matrix secretion and is characterized as a quantitative defect, i.e. as a deficiency in the amount or thickness of the enamel (see, for example,

Correspondence
Professor Horst Kierdorf, Department of Biology, University of Hildesheim, Marienburger Platz 22, 31141 Hildesheim, Germany.
T: +49 5121883913; F: +49 5121883911; E: kierdorf@rz.uni-hildesheim.de

Accepted for publication *10 March 2006*

Suckling et al. 1989; Goodman & Rose, 1990; Hillson, 1996, 2005). Enamel hypoplasia varies greatly in appearance. According to Berten (1895), three main types of hypoplastic enamel defects can be distinguished based on their macroscopic appearance: (1) pit-type defects – focal reductions of enamel thickness in the form of either isolated pits or groups of pits; (2) furrow-type defects – furrows running horizontally around the complete crown or parts of it – this type of defect being now mostly referred to as linear enamel hypoplasia (LEH); and (3) plane-type defects – extended areas of thinner than normal enamel.

In principle, this system of classification is still used today to characterize enamel defects caused by an impairment of enamel matrix formation (Commission on Oral Health, 1982; Hillson, 1996, 2005). More recently, so-called depressions have been described as a special type of LEH in porcine molar enamel (Dobney & Ervynck, 1998, 2000; Ervynck & Dobney, 1999, 2002; Dobney et al. 2002). The term was used for either shallow or deeper, horizontally orientated grooves with rounded edges, which are usually found in the cervical half of the lingual crown surface of M_1 and M_2 in pigs (Dobney & Ervynck, 1998).

Various factors have been identified as causing enamel hypoplasia. Factors of a systemic nature include dietary deficiencies, infectious diseases, intoxication, metabolic disorders and parasite infestation (Mellanby, 1929, 1930, 1934; Suckling et al. 1983, 1986; Suckling & Thurley, 1984; Goodman & Rose, 1990; Schroeder, 1991; Kierdorf et al. 1993, 1996, 2000, 2004; Psoter et al. 2005). It has been stressed that, regardless of the specific aetiology, developmental defects of enamel often result from a combination of one or more of these factors with normal physiological processes (Goodman & Rose, 1990; Brook et al. 1997; Larsen, 1997). So far it has not been possible to identify specific causes underlying the formation of specific types of enamel hypoplasia, and therefore hypoplastic enamel defects are employed as markers of generalized physiological stress during dental development (Hillson, 1996, 2005; Larsen, 1997).

The prevalence and intensity of enamel hypoplasia have been widely used to reconstruct health status, nutritional conditions, environmental influences, and social stress in past and present populations of humans and non-human primates (see Goodman & Rose, 1990; Hillson, 1996; Larsen, 1997; Hannibal & Guatelli-Steinberg, 2005). Recording of prevalence and intensity of enamel hypoplasia has further been applied as a useful tool for the reconstruction of the impact of stress factors, such as seasonal food shortage or weaning stress in various extant and extinct ungulate species (Dobney & Ervynck, 1998, 2000; Ervynck & Dobney, 1999, 2002; Mead, 1999; Dobney et al. 2002, 2004; Franz-Odendaal et al. 2003, 2004; Franz-Odendaal, 2004; Niven et al. 2004). In domestic pigs, the occurrence and intensity of enamel hypoplasia have been linked to different husbandry practices (Ervynck & Dobney, 1999), and the condition has even been used as an indicator for early domestication (Ervynck et al. 2002; Dobney et al. 2004).

Thus far, most studies on enamel hypoplasia have been restricted to the analysis of surface characteristics of teeth, as revealed by macroscopic inspection or examination using scanning electron microscopy. Only a few investigators have addressed the relationship between enamel microstructure and the macroscopic appearance of hypoplastic enamel defects. These studies demonstrated that by using this approach, additional information regarding the mechanisms of hypoplasia formation can be obtained (e.g. Rose, 1977; Goodman & Rose, 1990; Wright, 1990; Kierdorf et al. 1993, 1996, 2000, 2004; FitzGerald & Saunders, 2005). The aims of the present paper were, therefore: (1) to characterize the alterations of enamel microstructure in porcine teeth in relation to the macroscopic appearance of the different types of enamel hypoplasia; and (2) to reconstruct the reaction pattern of secretory ameloblasts on the basis of the observed deviations in enamel micromorphology. Special emphasis was laid on the characterization of 'depression-type' enamel defects. Depressions were first described in archaeological domestic pigs (Dobney & Ervynck, 1998) and have since also been recorded in prehistoric and recent populations of wild boar from different regions in Europe (Dobney et al. 2004). In the present study, teeth of archaeological domestic pigs and of recent wild boar were analysed.

Materials and methods

Permanent teeth exhibiting pit-type, furrow-type (LEH, including depressions) and plane-type enamel hypoplasia of different severity were obtained from a larger sample of complete or incomplete mandibular tooth rows of domestic pigs (*Sus scrofa* f. domestica) and from the mandibles of free-ranging wild boar (*Sus*

scrofa). The domestic pig material originated from the medieval archaeological site of Dryslwyn Castle in South Wales, UK, and most of it dated back to the 13th century. Dryslwyn Castle was the stronghold of the Lords of Dryslwyn and played an important role in the late 13th century history of Wales (Caple, 2002). The wild boar material was of recent origin and originated from animals that had been killed by hunters in the region of the Ore Mountains located on both sides of the border between Germany and the Czech Republic. It was previously demonstrated that the wild boar from this region exhibited varying degrees of dental fluorosis resulting from fluoride pollution of the environment (Kierdorf et al. 2000). Mandibular molars of domestic pigs from Dryslwyn Castle and of recent wild boar from a region near Cologne in western Germany, which on macroscopic inspection did not exhibit enamel defects, served as controls.

In total, 15 mandibular molars (M_1 and M_2) from 11 domestic pigs and 16 mandibular molars (M_1, M_2 and M_3), a mandibular second premolar (P_2), and a mandibular second incisor (I_2) from 11 wild boar were selected for microscopic analyses. Twenty-one of these teeth exhibited either only one or several different types of hypoplastic defect. The remaining 12 teeth (controls) were macroscopically free of enamel hypoplasia. All teeth were first inspected macroscopically and photographed (Minolta XG 9, Minolta, Osaka, Japan), and subsequently processed for microscopic study. For this, the teeth were embedded in epoxy resin (either Biodur®, Biodur products, Heidelberg, Germany, or Epofix®, Struers, Copenhagen, Denmark) and then sectioned axiobuccolingually through the highest point of the cusp, using an electric saw with a water-cooled diamond blade (Woko 50, Conrad Apparatebau, Clausthal-Zellerfeld, Germany).

For scanning electron microscopy, the cut surface of one of the resulting tooth blocks was polished and etched for 3–6 s with 34% (v/v) phosphoric acid. Specimens were then mounted on aluminium stubs, sputter-coated with gold or gold–palladium, and viewed in a scanning electron microscope (Hitachi S 520, Zeiss DSM 250 or Philips XL 20). For light microscopy, the cut surface of the other tooth half was polished and mounted on a glass slide. The mounted specimen was then sectioned to a thickness of approximately 300 μm, ground and polished to a final thickness of approximately 40 μm, and cover-slipped. The ground sections were viewed and photographed in transmitted light, using an Axioskop2 Plus microscope (Zeiss, Jena, Germany) equipped with a Canon Powershot G2 (Canon, Tokyo, Japan) digital camera. The acquired images were further processed with the software package Photoshop 7.0 (Adobe, San Jose, CA, USA).

Enamel thickness at different points along the corono-cervical tooth axis was measured at the lingual side of the distal tooth half of mandibular second molars with or without depressions, using assembled, scaled, low-magnification micrographs. For this purpose, intervals of 200 μm in the axial direction were marked at the dentine–enamel junction (DEJ), starting from the apical enamel border and proceeding in cuspal direction. The minimum distance from the DEJ to the enamel surface was then measured at each of the marked points, using the measurement tool within Photoshop. The value obtained represents the thickness of the enamel layer for the respective measurement point.

In seven M_2 (six from domestic pigs, one from a wild boar) showing depressions, the maximum depth of the defect was determined as the shortest distance between the deepest point of the depression and a tangential line connecting the crown surfaces located coronal and cervical to the depression (see Fig. 7b–d). A corresponding measurement was also taken in the cervical crown area of eight control M_2 (three from domestic pigs, five from wild boar), which on macroscopic inspection did not exhibit depressions (Fig. 7a). The assignment of the molars to either the control or the depression group was performed based on a macroscopic examination of the respective tooth surfaces by one of the authors (K.D.) prior to histological analysis.

Data for enamel thickness and depression depths were checked for normal distribution using the Komolgorov–Smirnov test. When the hypothesis of normality could be maintained, data were compared using Student's *t*-test. When the hypothesis of normality had to be rejected, data were compared with the Mann–Whitney non-parametric test. In all tests, two-sided P values < 0.05 were considered to indicate significance.

Results

On macroscopic inspection, the hypoplastic defects present in the enamel of the studied teeth could be classified as pit-type, plane-type or furrow-type (Fig. 1a–d,f).

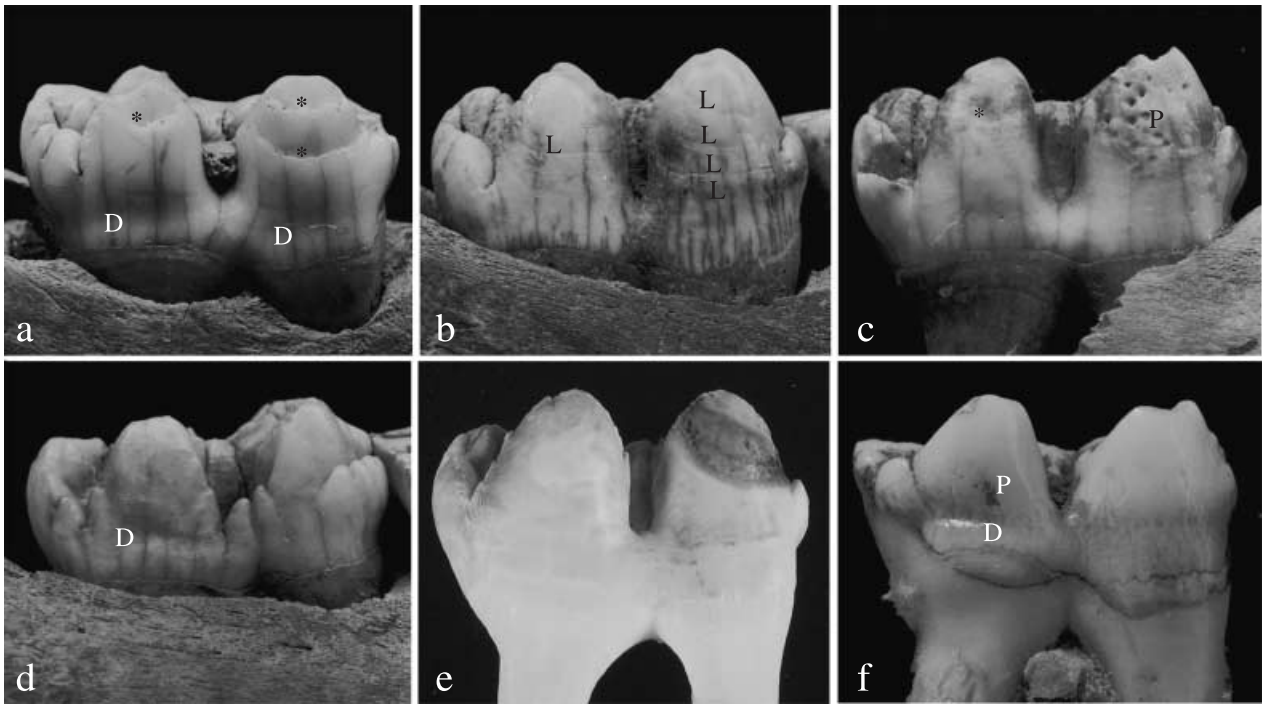

Fig. 1 Left (a–c) and right (d) M_2 of domestic pigs and left M_2 of wild boar (e,f) in lingual (a–c,e,f) or buccal (d) view. Different types of hypoplastic enamel defects are shown in a–d and f; e: control tooth. D = depression-type defects, L = linear (furrow-type) defects, P = pit-type defects, * = plane-type defects. Magnification approximately 2.5×.

Pit-type defects

Macroscopically, pit-type defects appeared as focal areas of reduced enamel thickness. The number of pits present in a tooth was highly variable, ranging from a single pit over a few clustered pits to many pits scattered over larger areas of the tooth crown (Fig. 1c,f).

Pits that reached deep into the enamel layer exhibited a funnel-shaped outline in the axiobuccolingual tooth sections (Figs 2a–c and 3a,c). A broad, strongly accentuated incremental line with a disruption of the normal prismatic enamel structure (Wilson band, pathological incremental band) was frequently associated with the defects. This pathological incremental band, which was observed in the enamel located cuspal and cervical to the defect, was continuous with the enamel surface at the bottom of the defect zone (Figs 2c and 3a–c). In acid-etched specimens viewed in the SEM, the pathological incremental band (or plane in three-dimensional view) sometimes appeared as a cleft (Fig. 3a–c). In other cases, a zone of aprismatic (prismless) enamel was found to be intercalated between a typically less severely accentuated incremental line and the bottom of the defect (Fig. 3d,e). The enamel surrounding the pit-type defects showed a bending of the striae of Retzius (regular long-period incremental markings) according to the outline of the defects (Fig. 2a,c). This bending was indicative of a gradual resumption of secretory activity by the ameloblasts that had produced the enamel forming the flanks of the pits. On tooth sections, it became evident that pits of similar extension at the crown surface could originate at different distances from the DEJ (Fig. 3b,c).

In an M_2 from a domestic pig, a single deep pit was partly filled with a mineralized deposit that contained lacunae with radiating canaliculi (Fig. 2c,d). The histological appearance of this deposit was that of coronal cementum. The enamel surface beneath this coronal cementum exhibited a scalloped outline, suggesting that enamel resorption had occurred prior to cementum deposition at this site (Fig. 2d).

Plane-type defects

Plane-type defects presented as extended areas of reduced enamel thickness (Figs 1a, 4a–d, 5a and 9a). Typically, the transition between the defect area and the cervically adjacent area of greater enamel thickness was marked by a distinct ledge. Sections through specimens with pronounced plane-type defects revealed

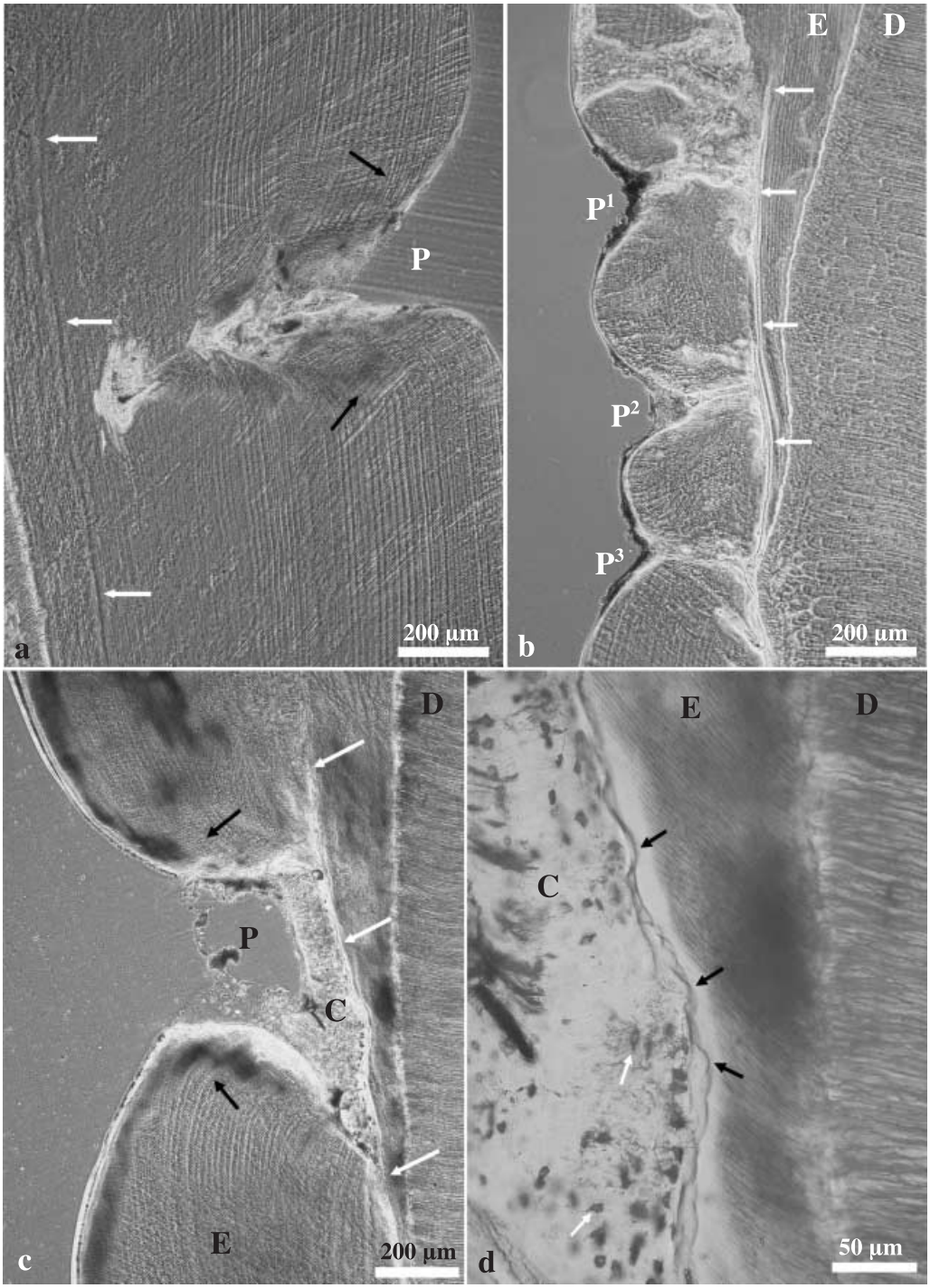

Fig. 2 Light micrographs of pit-type enamel defects. (a) Domestic pig, left M_2; longitudinal ground section through mesial tooth half, lingual enamel (phase contrast microscopy). Pit-type defect, note bending of the striae of Retzius in the enamel forming the wall of the defect (black arrows) and a pathological incremental band (white arrows) that is associated with the pit (P). (b) Wild boar, left M_1; longitudinal ground section through distal tooth half, lingual enamel (phase contrast microscopy). Three distinct hypoplastic pits (P1–3) originate at a pathological incremental band (white arrows). D = dentine, E = enamel. (c) Domestic pig, right M_2; longitudinal ground section through distal tooth half, lingual enamel (phase contrast microscopy). Large hypoplastic pit (P) in the enamel (E). The bottom of the defect is filled with cellular cementum (C). Note bending of the striae of Retzius (black arrows) in the enamel forming the wall of the defect. A pathological incremental band that is continuous with the enamel surface in the defect area can be seen (white arrows). D = dentine. (d) Higher magnification of the bottom area of the pit-type defect shown in (c) (bright-field microscopy). Note scalloped outline (black arrows) of the enamel (E) surface beneath the plug of cellular cementum (C) that contains numerous cementocyte lacunae (white arrows) with radiating canaliculi. D = dentine.

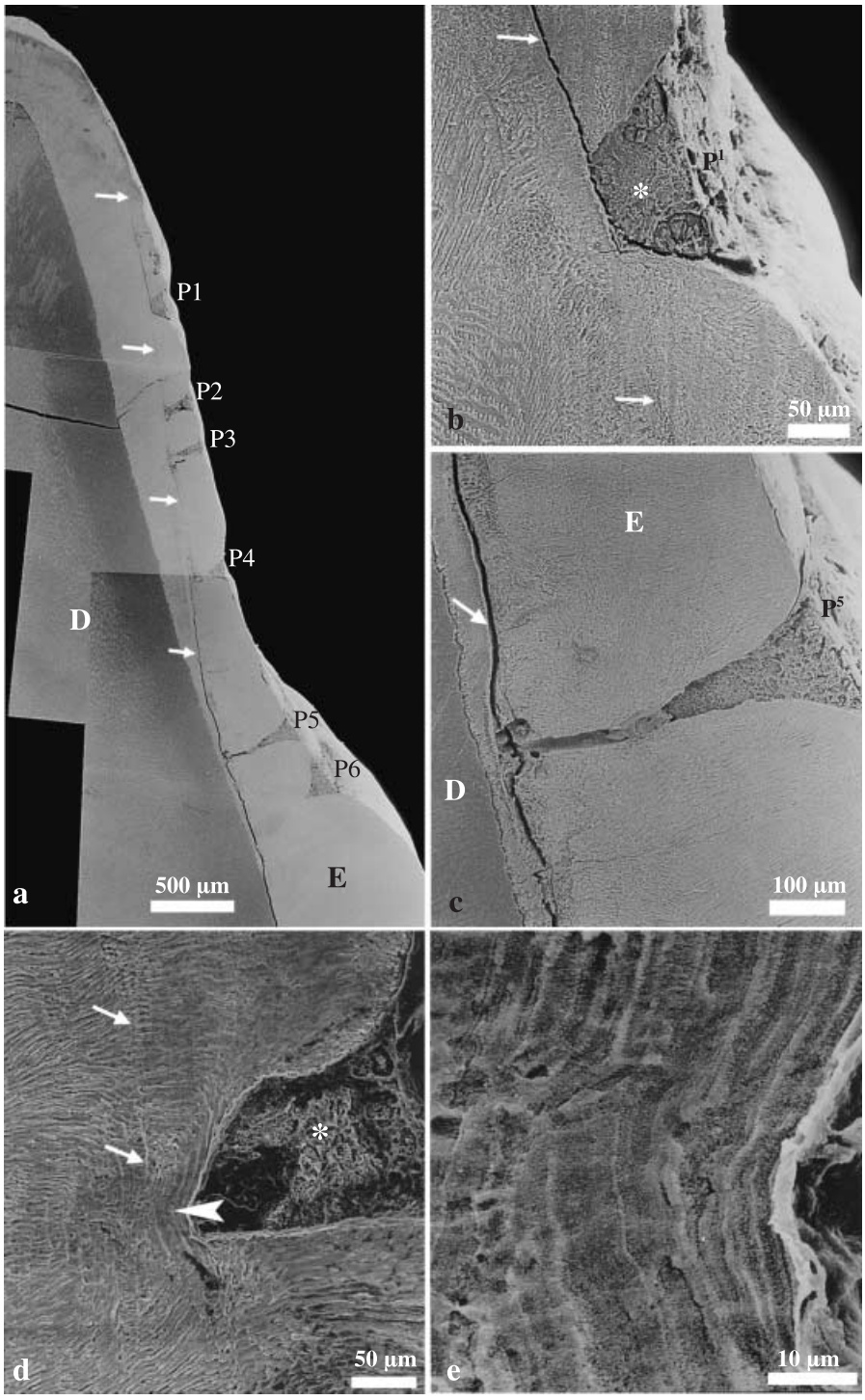

Fig. 3 Scanning electron micrographs of etched longitudinal sections through wild boar teeth. (a) Right P_2, buccal enamel. Row of pit-type hypoplastic enamel defects (P1–6) originating at a pathological incremental band (white arrows) that appears cleft-like. Defect P6 has been sectioned tangentially. D = dentine, E = enamel. (b) Higher magnification of the most cuspally located pit-type defect (P1) that is occluded by dental calculus (asterisk). Note pathological incremental band (white arrows) that is continuous with the bottom of the pit. (c) Higher magnification of pit P5, which extends deep into the enamel (E) and has a funnel-shaped sectional outline. The defect, which is partly filled by dental calculus, originates at a pathological incremental band (white arrow) that appears cleft-like. D = dentine. (d) Left I_2, labial enamel. Aprismatic enamel (arrowhead) beneath the base of a small pit-type hypoplastic defect that is filled with dental calculus (asterisk). A slightly accentuated incremental line is marked by arrows. (e) Higher magnification of aprismatic enamel beneath the bottom of the hypoplastic defect shown in (d). Note layered appearance of the aprismatic enamel.

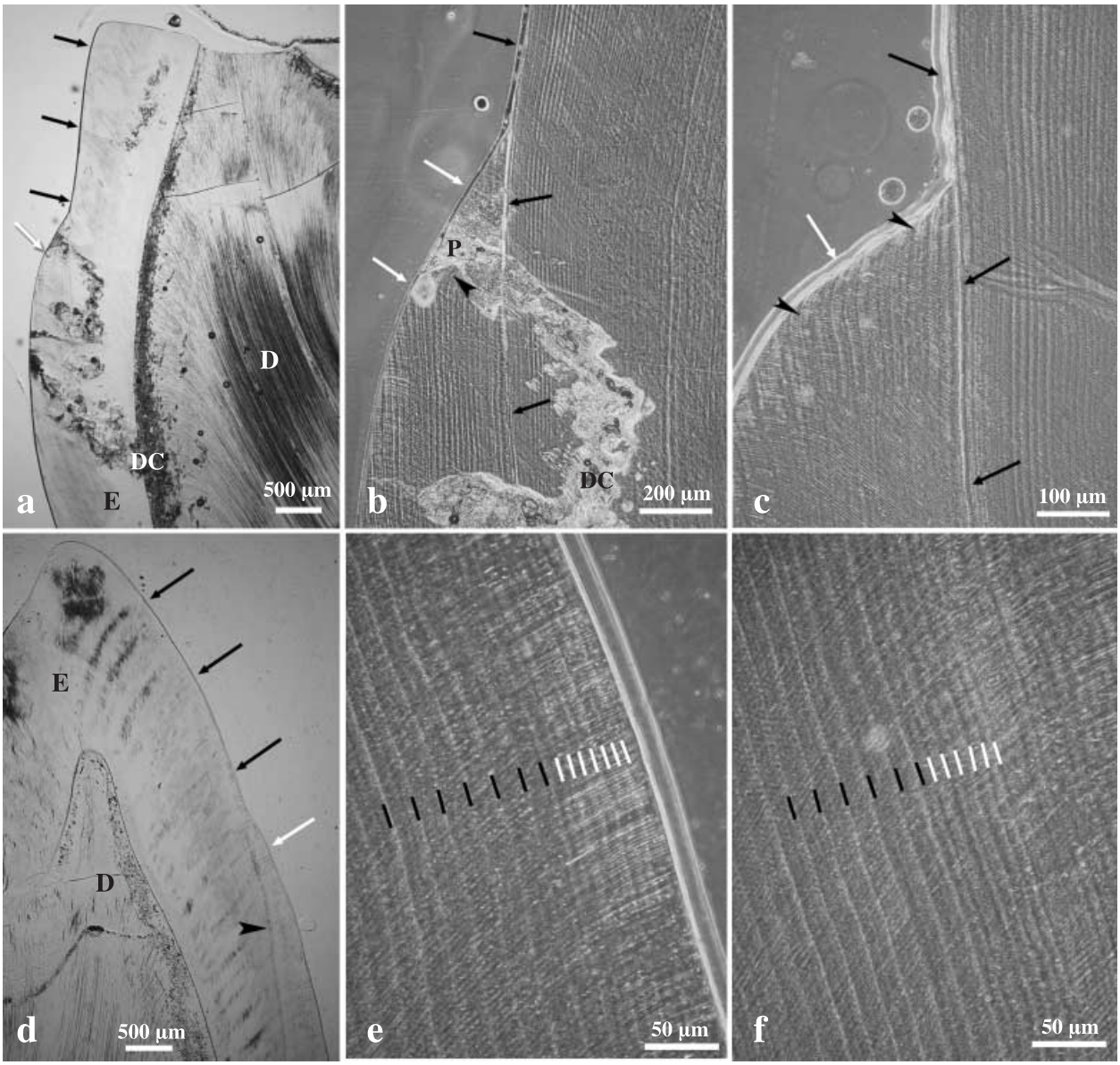

Fig. 4 Light micrographs of plane-type hypoplastic defects in the enamel of the left M_2 of domestic pigs, longitudinal ground sections; bright-field microscopy (a,d) or phase contrast microscopy (b,c,e,f). (a) Extended plane-type defect (black arrows). Ledge area (white arrow) located between the defect and the cervically adjacent enamel. D = dentine, DC = area exhibiting diagenetic changes, E = enamel. (b) Higher magnification of the ledge area shown in (a). A pathological incremental band (middle and lower black arrows), which is continuous with the enamel surface of the defect area (upper black arrow), is present in the enamel cervical to the defect. A single pit-type defect (P) is present in the ledge area (white arrows). Note bending of the striae of Retzius (arrowhead) according to the outline of the pit. DC = area exhibiting diagenetic changes. (c) Ledge area (white arrow) located cervical to a plane-type defect (upper black arrow) that is continuous with a pathological incremental band (middle and lower black arrows). Note bending of the striae of Retzius in the outer enamel of the ledge area (arrowheads). (d) Shallow plane-type defect (black arrows) cuspal to a less pronounced ledge (white arrow). A group of narrow spaced striae of Retzius (arrowhead) can be seen in the enamel cervical to the ledge. D = dentine, E = enamel. (e) Higher magnification of the enamel surface of the hypoplastic defect near the ledge area shown in (d). A group of narrow spaced striae of Retzius (marked in white) is visible in the enamel directly beneath the enamel surface. The striae of Retzius located deeper in the enamel (marked in black) show a normal spacing. (f) Higher magnification of the enamel located cervical to the defect area. The group of narrow spaced striae of Retzius (marked in white) is located deeper within the enamel. Normally spaced striae of Retzius internal to this band are marked in black.

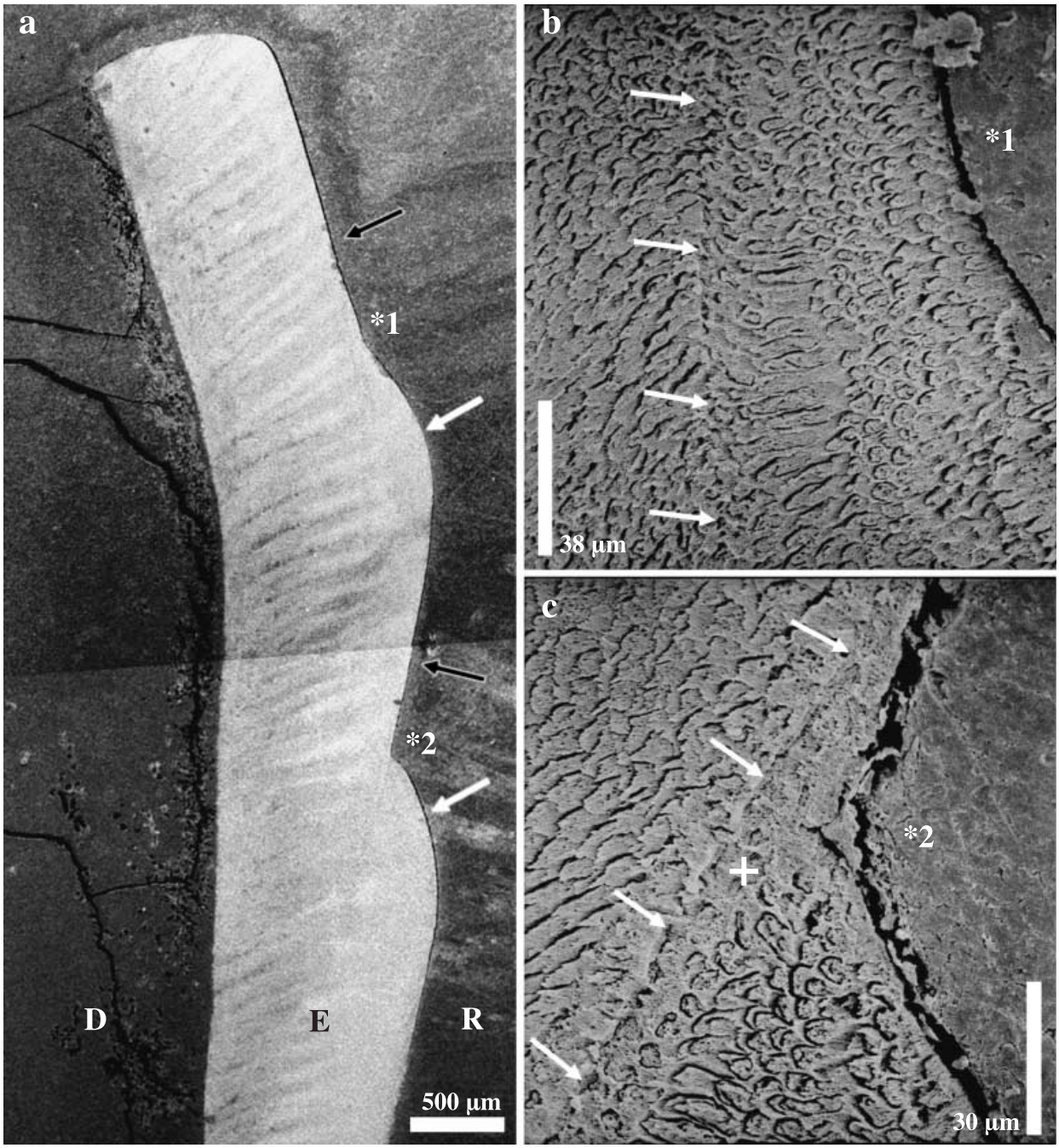

Fig. 5 Scanning electron micrographs of etched longitudinal sections through lingual enamel of the left M_2 of a domestic pig. (a) Two plane-type defects (black arrows) can be seen. Distinct ledges (white arrows) are present cervical to these defects. Note the more obtuse angle between the exposed incremental plane and the ledge in the cuspal (*1) compared with the cervical (*2) defect. D = dentine, E = enamel, R = resin. (b) Higher magnification of the defect marked by *1 in (a). White arrows point to a pathological incremental band. (c) Higher magnification of the defect marked by *2 in (a) and the associated pathological incremental band. Note sharp demarcation of this band (white arrows) against the enamel located internal to it and zone of aprismatic enamel (+) intercalated between the demarcation line and the prismatic enamel located further peripherally.

that they were regularly associated with the presence of a pathological incremental band (Figs 4b,c and 5). This band occurred in the enamel located cervical to the ledge and was continuous with the enamel surface in the defect area. The position of the pathological incremental band and the enamel surface in the defect area indicated the location of the enamel-forming front at the time of a severe impact on the secretory

ameloblasts. In teeth presenting multiple plane-type defects, the angle between the enamel surface in the defect area and the ledge was more obtuse in cuspally located compared with more cervically located defects (Fig. 5a).

In the SEM it became apparent that the pathological incremental band was sharply demarcated from the prismatic enamel located internal to it (Fig. 5b,c). Towards the enamel surface, a zone of aprismatic enamel was often intercalated between the demarcation line against the inner prismatic enamel and the again prismatic enamel located further peripherally (Fig. 5c). The striae of Retzius in the outermost enamel of the ledge area exhibited a bending corresponding to the outline of the enamel surface (Fig. 4c). In one specimen, small pit-type defects occurred in the ledge area. The bases of these pits were located at the pathological incremental band (Fig. 4b).

In another specimen with a macroscopically less pronounced plane-type defect, no pathological incremental band was observed in the enamel. Instead, a group of striae of Retzius with a reduced spacing was associated with the defect (Fig. 4d–f).

Furrow-type defects (LEH)

These defects appeared as furrows running in a horizontal direction around the entire tooth crown or parts of it (Fig. 1b). In its slightest form, the defect presented only as a minor accentuation of a single or a few adjacent perikyma grooves. Microscopic examination of tooth sections revealed that in the studied specimens this type of enamel defect was not associated with the presence of a pathological incremental band or other marked deviations from normal enamel microstructure (Fig. 6a–c). Instead, the presence of linear enamel defects could be related to an increased spacing between adjacent perikyma grooves in the occlusal wall of the defect, resulting in a larger than normal incremental plane [or stria of Retzius plane according to Hillson & Bond's (1997) terminology] being exposed at the tooth surface (Fig. 6c). This indicated that in these areas, a larger than normal number of ameloblasts had prematurely and simultaneously ceased matrix production. Therefore, the number of prisms ending at or near (in the case of the final enamel being aprismatic) the enamel surface within the affected increments exceeded that in the cuspally and cervically adjacent, less affected or unaffected increments (Fig. 6c). The perikyma ridges located cervical to the defect were slightly more pronounced than those located cuspal to the defect (Fig. 6c), resulting in a slight increase in enamel thickness (Fig. 9a).

Depressions as a special form of LEH

On macroscopic inspection, depressions were characterized as broad, horizontally orientated shallow grooves (Fig. 1a,d,f). They occurred almost exclusively in the cervical half of the lingual crown surfaces of the inspected molars and were typically more pronounced on the lingual surface of the distal than that of the mesial crown portion of an individual tooth (Fig. 1a,d,f).

On sections through teeth classified as exhibiting depression-type hypoplasia based on macroscopic inspection, it was observed that – corresponding to the concavity of the enamel surface – a concavity also occurred in the course of the DEJ (Fig. 7b–d). The deepest point of the concavity along the DEJ was located slightly more cuspally than the deepest point of the enamel surface. A flattening or slight depression of the lingual enamel surface was, however, often also discernible in the cervical crown area of control molars, i.e. of molars diagnosed as not exhibiting depression-type hypoplasia on macroscopic inspection (Fig. 7a). Measurement at corresponding points along the coronal–cervical tooth axis revealed significantly lower enamel thickness in M_2 classified as exhibiting depression-type defects compared with control M_2 (Fig. 9b). Typically, the difference in enamel thickness between controls and affected molars gradually increased from the mid-crown area in a cervical direction, reaching a maximum at the deepest point of the DEJ. Further cervically, the difference in enamel thickness gradually decreased, with a minor, but still significant difference remaining at the level of the cementum–enamel junction (Fig. 9b).

Maximum depression depth (mean 105 μm, range 43–172 μm) in the control M_2 ($n = 8$) was significantly lower (t-test: $t = -7.288$, d.f. = 13, $P < 0.00001$) than depression depth (mean 347 μm, range 269–491 μm) in the M_2 ($n = 7$) classified as presenting depression-type defects.

Light and scanning electron microscopic analysis of the enamel in the depression area revealed no indications of a markedly disturbed micromorphology, i.e. of pathological incremental bands with disruption of the

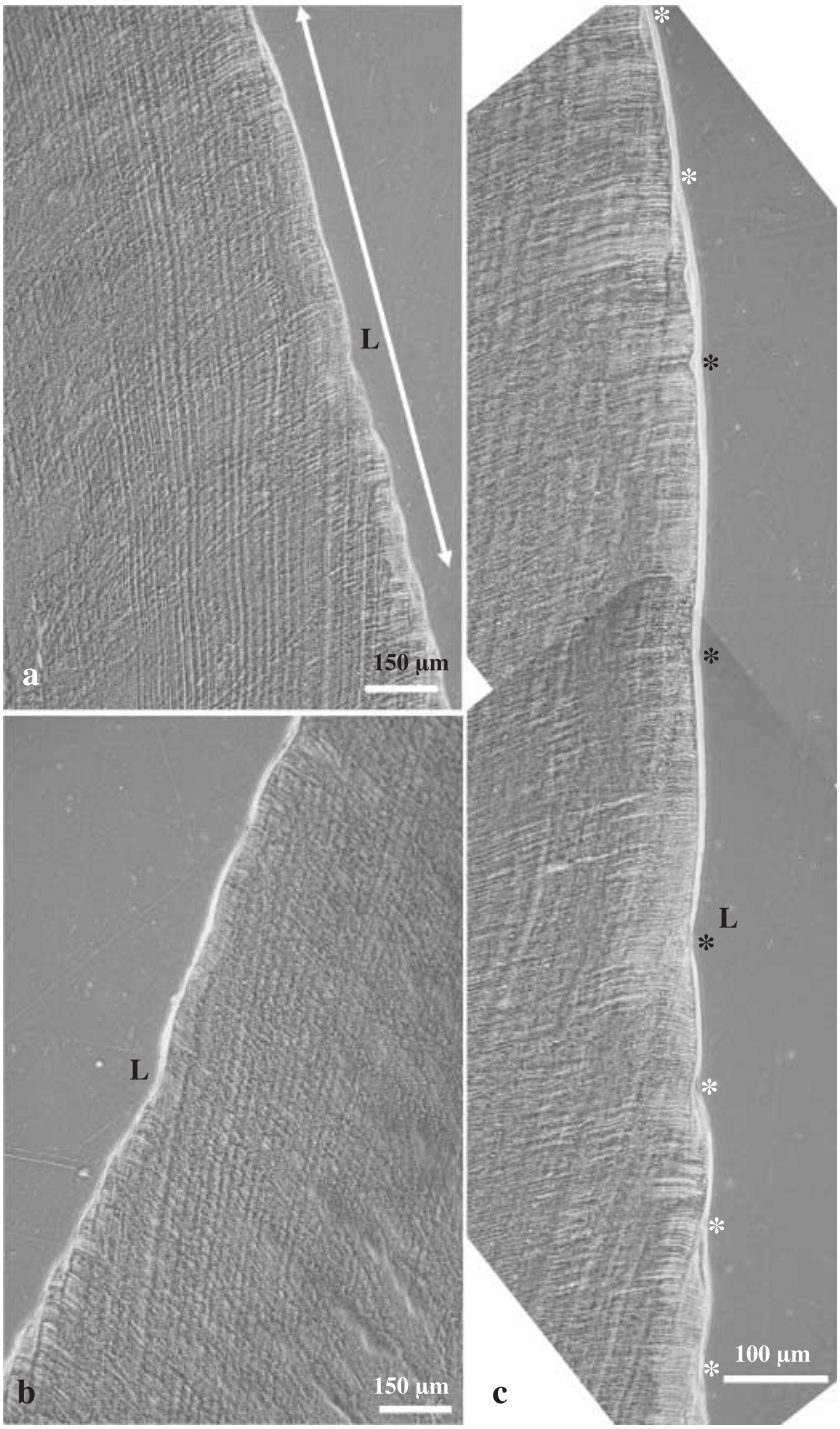

Fig. 6 Light micrographs (phase contrast microscopy) of a longitudinal ground section through a left M_2 of a domestic pig. (a) Linear hypoplastic defect (L) in lingual enamel. The double headed arrow denotes the area magnified in (c). (b) Corresponding linear defect (L) in buccal enamel. (c) Higher magnification of the area marked in (a). Perikyma grooves are marked by asterisks. Note increased distance between three neighbouring perikyma grooves (black asterisks) in the occlusal wall of the defect. White asterisk: normally spaced perikyma grooves.

prismatic enamel structure or zones of aprismatic enamel (Fig. 8). The course of the striae of Retzius showed a bending according to the concavity in the DEJ and the outline of the enamel surface (Fig. 7b–d). However, compared with corresponding enamel areas of control teeth, a reduced spacing between the striae of Retzius was observed in the enamel underlying the depressions (Fig. 8a–e). Moreover, in the SEM a slight accentuation, i.e. increased visibility, of the incremental markings (both striae of Retzius and shorter-period incremental markings) was noted in these enamel areas (Fig. 8g). The shorter-period incremental markings were visible as prism cross-striations and, in interprismatic and aprismatic enamel, as features resembling

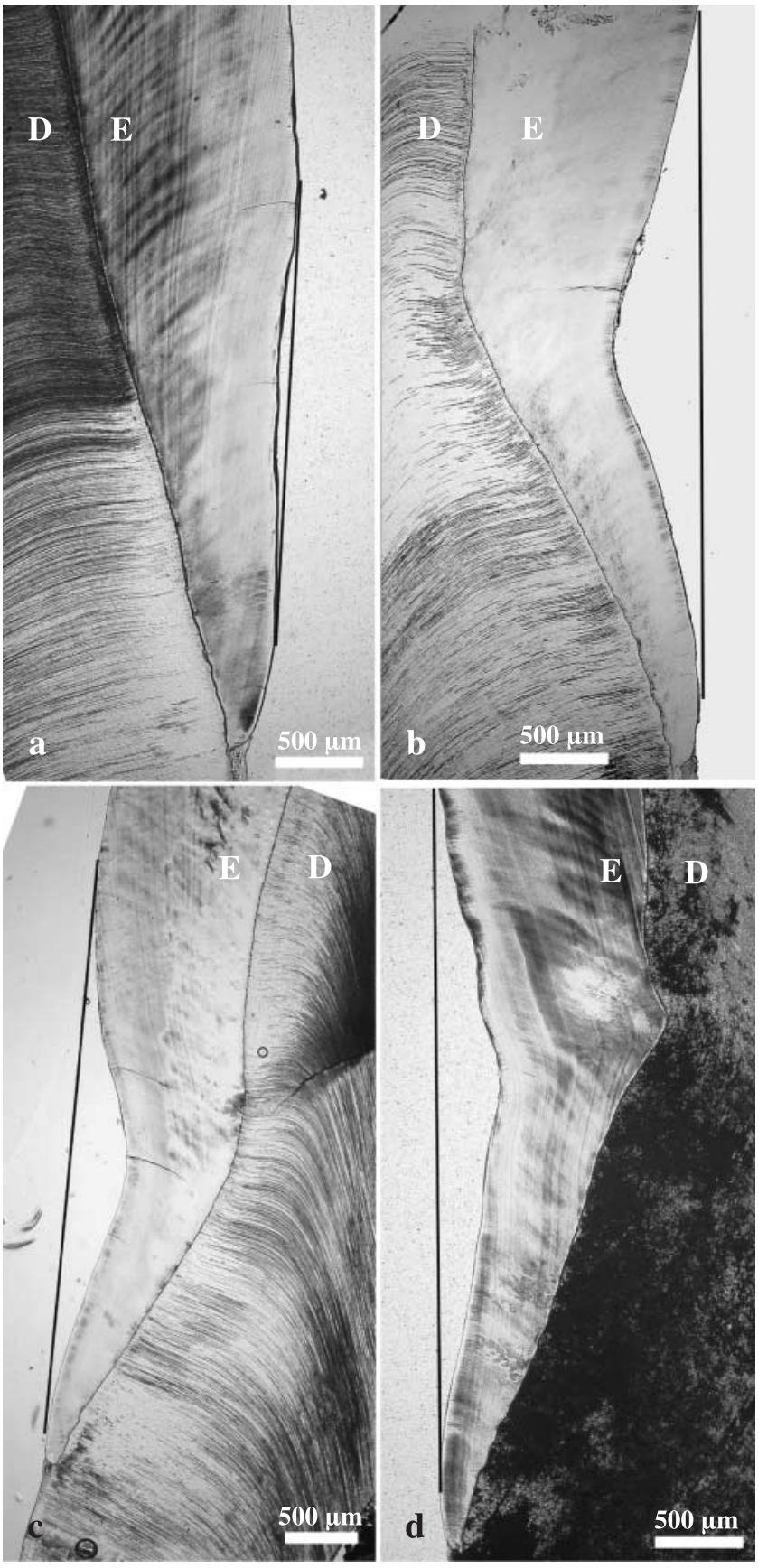

Fig. 7 Light micrographs (bright-field microscopy) of longitudinal ground sections through lingual enamel of the distal half of M_2 from wild boar (a,b) and domestic pigs (c,d). (a) Control molar exhibiting a very slight concavity in the cervical enamel surface. The shortest distance between the deepest point of the concavity of the enamel surface and the tangential line connecting the cuspally and cervically adjacing enamel surfaces is 65 μm. (b–d) Molars exhibiting depression-type defects. Note distinct concavity of both the cervical enamel surface and the course of the DEJ. Maximum depression depth is 491 μm in (b), 388 μm in (c) and 373 μm in (d). D = dentine, E = enamel.

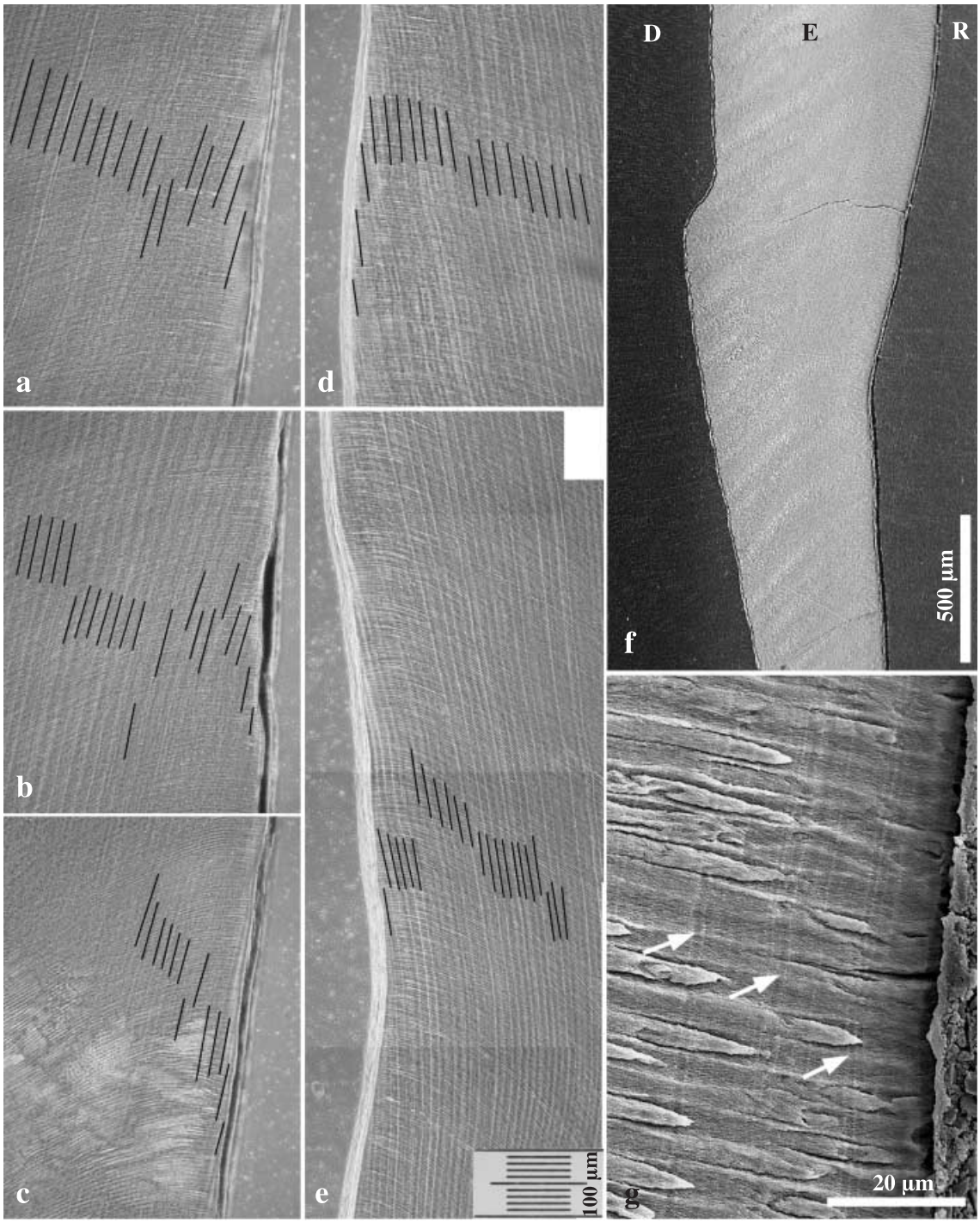

Fig. 8 Light and scanning electron micrographs of longitudinal sections through porcine molar enamel. (a–e) Light micrographs (phase contrast microscopy) of ground sections through lingual enamel of the distal half of M_2 from a wild boar (a–c) without depression-type defect and a domestic pig (d,e) exhibiting a depression-type defect. Mean distances between neighbouring striae of Retzius (marked in black) in the control molar were *c.* 24 µm in cuspal (a), *c.* 19 µm in mid-crown (b), and *c.* 16 µm in cervical enamel (c). In the M_2 with a depression-type defect, the distances between neighbouring striae of Retzius (marked in black) were *c.* 20 µm in cuspal enamel adjacent to the depression area (d) and *c.* 12 µm in the surface enamel at the deepest point of the depression (e). (f,g) Scanning electron micrographs of etched longitudinal sections through the lingual enamel of a domestic pig M_2 exhibiting a depression-type defect. (f) No marked disturbance of enamel microstructure is discernible in the depression area. D = dentine, E = enamel, R = resin. (g) Higher magnification of the surface enamel at the deepest point of the depression depicted in (f). Note slight accentuation of the striae of Retzius (arrows) and of shorter-period incremental markings in both enamel prisms and interprismatic/aprismatic enamel.

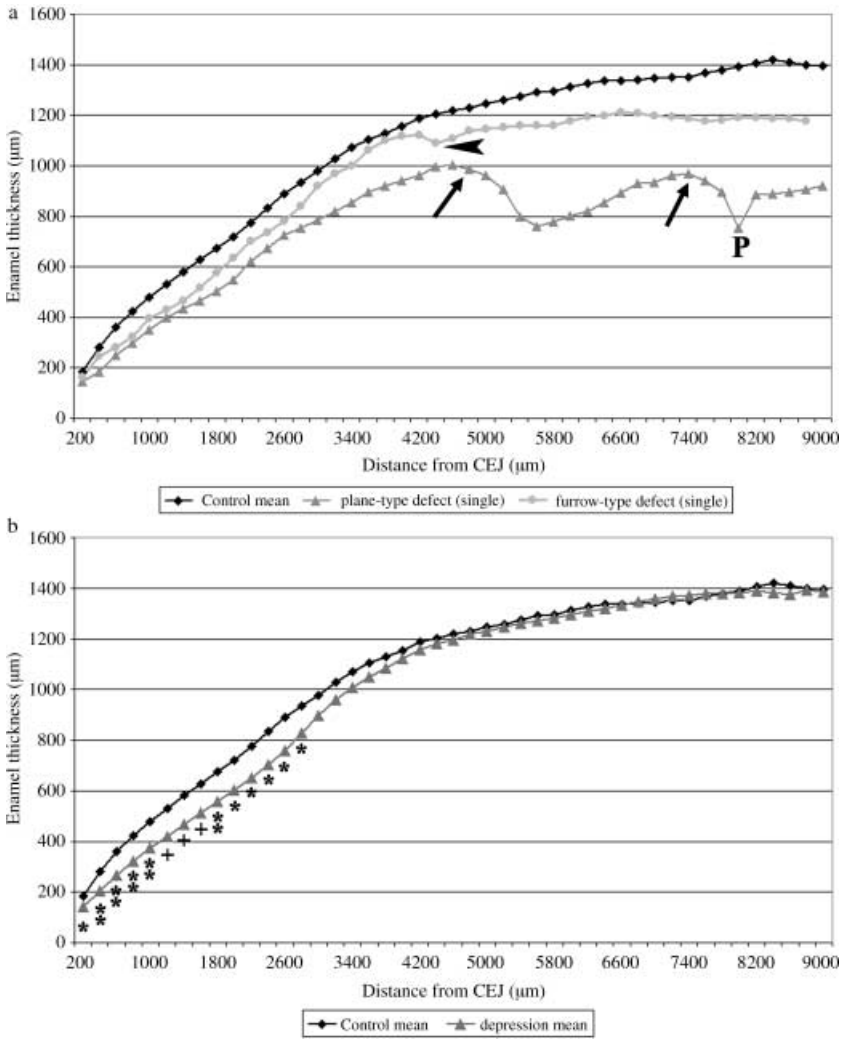

Fig. 9 Results of enamel thickness measurements. (a) Comparison of lingual enamel thickness in control M_2 (mean of eight specimens, upper curve), in a single M_2 exhibiting a furrow-type defect (LEH, middle curve) and in another M_2 showing two plane-type hypoplastic defects (lower curve). Note grossly reduced thickness of cuspal enamel in the tooth exhibiting the two plane-type defects. Ledges located cervical to these defects are marked by black arrows. The two defects are shown in Figs 1(a) and 5(a). P = pit-type defect located in ledge area. In the tooth exhibiting LEH, the arrowhead indicates the furrow marked by 'L' in Fig. 6(c). (b) Comparison of enamel thickness between control M_2 (n = 8) and M_2 (n = 7) classified as exhibiting depression-type defects. Significant differences of enamel thickness at corresponding distances from the CEJ are marked (*P < 0.05, **P < 0.01, Student's t-test; ^{+}P < 0.05, Mann–Whitney U-test).

the 'laminated striations' or 'laminations' described, respectively, by Kodaka et al. (1991) for human enamel and by Smith (2006) for primate enamel.

Discussion

Our study demonstrated a wide variety of developmental defects in the enamel of porcine teeth. The different types of macroscopically defined hypoplastic defects were associated with different microstructural alterations of the enamel.

Several studies have shown that deviations of enamel microstructure in teeth of mammals can be related to specific changes in the morphology and function of the secretory ameloblasts (Walton & Eisenmann, 1974; Suckling et al. 1988, 1989; Monsour et al. 1989; Kodaka et al. 1991, 1995; Kierdorf et al. 1993, 1996, 2000, 2004; Wöltgens et al. 1995; Kierdorf & Kierdorf, 1997). Therefore, alterations in enamel microstructure can be used to reconstruct the intensity and duration of impacts on these cells.

Each ameloblast possesses a cytoplasmic extension at its distal end, the so-called Tomes' process. During initial enamel formation, the Tomes' process comprises only a proximal portion, and matrix secretion takes place at its single secretory surface. With increasing secretory activity of the ameloblast, the Tomes' process elongates, leading to the formation of the distal or interdigitating portion of the process (Boyde, 1967, 1989, 1997; Warshawsky et al. 1981; Warshawsky, 1988; Nanci, 2003). In consequence, the secretory ameloblast now possesses two secretory surfaces that are orientated at a certain angle to each other, a fact that causes the characteristic microstructural organization of mammalian enamel. This structure consists of prisms (or rods), which are formed in the matrix secreted at

the secretory surface of the distal portion of the Tomes' process, and interprismatic (inter-rod) enamel, which is formed in relation to the secretory surface of the proximal portion of the Tomes' process (Boyde, 1967, 1989, 1997; Warshawsky et al. 1981; Warshawsky, 1988; Nanci, 2003). Maintenance of this ameloblast morphology requires a continuous high secretory activity of the cell (Warshawsky & Vugman, 1977). Towards the end of enamel matrix formation, the secretory activity of ameloblasts normally gradually decreases. When the secretory activity falls below the threshold necessary for maintaining the distal portion of the Tomes' process, a thin surface zone of aprismatic enamel is laid down by the ameloblasts. Final enamel, like initial enamel, is therefore frequently aprismatic (Boyde, 1967, 1989, 1997; Warshawsky et al. 1981; Warshawsky, 1988; Sasaki et al. 1997; Nanci, 2003).

Enamel formation starts at the cusp tip(s) of a tooth and proceeds in a cervical direction as a result of successive recruitment of new cohorts of secretory ameloblasts. Thus, for any given time during the secretory stage of amelogenesis, more cuspally located secretory ameloblasts are in a later stage of their secretory activity than those located more cervically. A systemic disturbance during the secretory stage of amelogenesis therefore hits ameloblasts in different phases of their secretory activity.

The deviations from normal enamel microstructure observed in porcine teeth with enamel hypoplasia can be interpreted as representing a continuum of increasingly more severe disturbance of enamel matrix formation. This indicates a graduated response of secretory ameloblasts to pathophysiological impacts of different intensity and duration.

If changes in enamel microstructure are limited to an overall enhancement of the incremental pattern (striae of Retzius and shorter period incremental markings) and a reduced spacing between striae of Retzius, but the prismatic structure of enamel is maintained, impairment of secretory cell function has been below the threshold causing a complete reduction of the distal portion of the Tomes' processes of the ameloblasts.

Formation of the normal pattern of striae of Retzius has been related to a periodic constriction at the base of the distal portion of the Tomes' process during periods of reduced secretory activity, leading to an expansion of the interprismatic at the expense of prismatic enamel and a resulting periodic constriction of the prism (Risnes, 1990, 1998). Several studies have demonstrated an overall enhancement of the incremental pattern as a result of a disturbance of enamel formation owing to various causes (Mellanby, 1929, 1930, 1934; Gustafson & Gustafson, 1967; Fejerskov et al. 1977; Goodman & Rose, 1990; Condon & Rose, 1992; Suga, 1992; Kierdorf & Kierdorf, 1997; Kierdorf et al. 2000, 2004). It has therefore been suggested that an overall enhancement of the incremental pattern occurs due to a pathological intensification of the rhythmic secretion of the enamel matrix, i.e. of a more pronounced constriction at the base of the distal portion of the Tomes' process than normal due to moderate stress acting on the ameloblast (Risnes, 1998; Kierdorf et al. 2000).

Abnormal zones of aprismatic enamel denote a more severe impairment of secretory function that led to a temporary or permanent reduction of the distal portion of the Tomes' process in the affected ameloblasts. However, secretion continued at a low rate at the single, flat, secretory surface of the Tomes' process. The layered appearance of this aprismatic enamel indicates that, despite the overall reduction of secretory activity, a rhythmic nature of enamel matrix secretion was maintained. This phenomenon has previously been described in fluorotic enamel of deer (Kierdorf et al. 1993, 1996; Kierdorf & Kierdorf, 1997) and in prismless enamel of human teeth (Kodaka et al. 1991, 1995).

The presence of a pathological incremental band in the enamel is interpreted as reflecting a severe reduction or temporary cessation of enamel matrix formation (Kierdorf & Kierdorf, 1997; Kierdorf et al. 2000, 2004). Occurrence of a zone of disturbed enamel structure external to this band indicates that it took some time for the ameloblasts to re-establish their normal secretory activity and the related Tomes' process morphology. If such a pathological incremental band is continuous with parts of the enamel surface, no resumption of secretory activity had occurred in the latter locations. In these cases the enamel surface corresponds to an exposed incremental plane or stria of Retzius plane (Hillson & Bond, 1997). When the outermost enamel at the bottom of a hypoplastic defect shows a prismatic structure, it can be deduced that matrix secretion had stopped abruptly and definitely (Boyde, 1970; Kierdorf & Kierdorf, 1997).

As has been discussed by Hillson & Bond (1997), the macroscopic appearance of hypoplastic enamel defects is dependent on: (1) the intensity and duration of the insult and the corresponding reaction of the secretory

ameloblasts; (2) the number of secretory ameloblasts affected by the insult; (3) the position of the affected ameloblasts along the corono-cervical tooth axis and the corresponding time elapsed from entering into the secretory stage; and (4) the species- and tooth-specific geometry of crown growth.

In the case of pit-type hypoplastic defects, a group of ameloblasts stopped matrix production, while neighbouring ameloblasts were able to continue secretion. The causes underlying this variation in the reaction of neighbouring ameloblasts are unknown. Resumption of secretory function typically increased with distance from the defect, as was evidenced by the bending in the course of the striae of Retzius in the enamel forming the walls of the pits. This bending of the striae of Retzius allows a distinction between hypoplastic defects and defects caused by post-eruptive loss of enamel (Kierdorf et al. 1993, 1996, 2000), a point not mentioned by Hillson & Bond (1997) in their seminal paper on the development of hypoplastic defects in human enamel.

Pit-type hypoplastic defects reaching deep into the enamel typically appeared funnel-shaped. This can hypothetically be related to two facts. First, in the bulk of the enamel the prisms follow an undulating course with the amplitude increasing peripherally. In consequence, the volume occupancy of a group of prisms increases in a peripheral direction (Radlanski, 1998). Second, the recovery of secretory ameloblasts that form the enamel of the flanks of the hypoplastic pits is a graduated one, as is evidenced by the bending of the striae of Retzius in these areas.

In the case of plane-type hypoplastic defects, ameloblasts, being in a later phase of their secretory activity, permanently stopped matrix production, while more cervically located ameloblasts, being at earlier phases of matrix secretion, resumed their secretory activity following the insult or were unaffected. An increased vulnerability of late secretory ameloblasts to stress has previously been reported by Suckling & Thurley (1984) for sheep. The bending of the striae of Retzius in the outermost enamel of the ledge area is indicative of a gradual resumption of secretory activity of the ameloblasts in this transitional zone and, as mentioned for pit-type defects, allows a distinction between hypoplastic defects and lesions resulting from post-eruptive enamel loss. Such post-eruptive tissue loss has been reported to occur along severely hypomineralized pathological incremental bands in fluorotic enamel (Fejerskov et al. 1994, 1996; Kierdorf et al. 1996, 2000). In these cases, a secretory-stage defect predisposes a certain area of the enamel to damage during the period of tooth function.

As has already been emphasized by Hillson & Bond (1997), in addition to the number of ameloblasts ceasing matrix production, the extension of a plane-type hypoplastic defect is also dependent on the geometry of crown growth, i.e. on the number of ameloblasts that are secretorally active at a given time and the related orientation of the enamel-forming front. Thus, for example, an acute angle between the striae of Retzius and the DEJ indicates that more ameloblasts had been simultaneously active at a given time than in cases where the striae of Retzius follow a more horizontal course (Dean & Wood, 1981). In porcine enamel, the inclination of the striae of Retzius is generally rather steep, with the steepness increasing in cuspal direction. In human enamel, the striae of Retzius follow a less steep course than in porcine enamel (C. Witzel et al. unpublished data). In defects located at corresponding crown heights, an exposed incremental plane in human enamel therefore forms a less obtuse angle with the cervically located ledge than in porcine enamel. Furthermore, within a species a disturbance of ameloblast function of similar intensity and duration will produce a more wedge-shaped defect in cervical compared with more cuspal enamel.

The steep inclination of the exposed incremental planes in plane-type defects of porcine enamel may lead to a misclassification as LEH on the basis of a purely macroscopic analysis. Thus, some of the defects previously described as LEH by Dobney & Ervynck (1998) in domestic pigs are in fact plane-type defects.

The results of the present study corroborate Hillson & Bond's (1997) conclusion that LEH results from a larger than normal group of late secretory ameloblasts ceasing matrix production along a single or multiple perikyma grooves. In consequence, in these cases a larger than normal number of prisms terminate in the occlusal wall of the furrow. In the material analysed in the present study, occurrence of LEH was not associated with the presence of a pathological incremental band.

With regard to the depression-type defects described by Dobney & Ervynck (1998), the present study revealed that the external appearance of these defects results from a combination of two phenomena. These are a distinct concavity of the DEJ in the cervical crown area

of a tooth, and a reduced enamel thickness in that area. Both factors contribute to the significantly increased depths of the concavity in the lingual enamel of molars diagnosed to show the phenomenon. The present study demonstrates that the development of the depression-type defects represents an abnormal enhancement of a regularly occurring phenomenon, namely a flattening or minor concavity in the lingual enamel of pig molars. It therefore seems justified to regard depressions as a pathological phenomenon, as was originally suggested by Dobney & Ervynck (1998). From our data it appears that by macroscopic inspection of tooth crowns, depressions in the enamel surface can be diagnosed if their depth exceeds about 200 μm.

On SEM inspection, the only micromorphological alterations in the otherwise normally structured enamel of the depression area were, however, a slight accentuation of the incremental pattern and a reduced spacing of the striae of Retzius, the latter indicating a reduction in the rate of enamel matrix secretion over an extended period of time. Apparently, the disturbance of enamel matrix secretion leading to depression-type defects stayed below the threshold that would have caused a complete reduction of the distal portion of Tomes' processes of the affected ameloblasts. The histological findings of the present study point to minor or moderate stress as a factor involved in the formation of the depressions and are thus in principle consistent with the hypothesis that the depressions in porcine enamel reflect a prolonged period of undernutrition of the pigs (Dobney & Ervynck, 1998; Ervynck & Dobney, 1999, 2002).

In human enamel, Wright (1990) likewise reported the presence of shallow hypoplastic defects in the absence of Wilson bands. Wright also assumed that this type of defect is caused by prolonged periods of mild stress, which negatively affects the secretory activity of the ameloblasts, but does not surpass the threshold necessary for the formation of Wilson bands. With respect to our observations in porcine enamel it must, however, be emphasized that the course of the DEJ, which deviated from normal in the teeth exhibiting depressions, is already fixed prior to the onset of enamel formation (Nanci, 2003), and thus cannot be related to the assumed period of undernutrition during later life. The cause for this deviation in the course of the DEJ in the affected pig teeth is unknown.

The presence of coronal cementum in a pit-type hypoplastic defect was observed in one tooth from a domestic pig. Coronal cementum is not normally formed in pig teeth, and its occurrence indicates a pathological, premature disintegration of the reduced enamel epithelium. In consequence, cells of the dental follicle could come into contact with the surface of the immature enamel and subsequently differentiate into cementoblasts (Diekwisch, 2001). Deposition of coronal cementum onto hypoplastic enamel has previously been documented in fluorotic teeth of wild boar (Kierdorf et al. 2005). In the horse, in which coronal cementum is regularly formed, cementum deposition is preceded by enamel resorption by odontoclasts, presumably to achieve a better attachment of the cementum to the enamel surface (Jones & Boyde, 1974). Interestingly, a scalloped outline of the enamel surface, resembling resorption lacunae, was also seen in the pig tooth, which suggests a similar sequence of events as occurs physiologically in the horse.

In conclusion, this study has revealed that the microscopic analysis of enamel structure in porcine teeth showing enamel hypoplasia allows an assessment of the intensity and duration of stress events affecting secretory ameloblasts. Pit-type and plane-type defects denote a severe impact of shorter duration on the secretory ameloblasts. By contrast, depressions are indicative of a longer lasting but less intense impairment of secretory ameloblast function. Linear defects are the result of premature cessation of matrix secretion by a cohort of late secretory ameloblasts. Thus, within the spectrum of enamel hypoplasia observed in the pig teeth, linear defects represent the least severe form. Based on an understanding of the normal morphology and function of ameloblasts, it is possible to relate the morphological alterations in enamel observable at the macroscopic and microscopic levels to changes at the cellular level. Microscopic analysis of enamel structure thus provides a deeper insight into the mechanisms underlying the formation of developmental defects in enamel than can be achieved by mere inspection of tooth surface characteristics alone.

Acknowledgements

This study was supported by Wellcome Trust Bioarchaeology Fellowships to K.D. (grant references 060888 and 071037), a research grant by the Arts and Humanities Research Board (award reference no. B/RG/AN1759/APN10977), the Flemish Heritage Institute, and the Research Commission of the University of Hildesheim.

We are also grateful to Dr Chris Caple (University of Durham) for providing (and allowing sectioning of) selected archaeological pig teeth from Dryslwyn Castle, Wales, and to Professor M. Schultz, M. Brand and I. Hettwer-Steeger (University of Göttingen) and Dr M. Hardt and S. Agel (University of Giessen) for providing access to SEM facilities and preparation of some ground sections.

References

Berten J (1895) Hypoplasien des Schmelzes (Congenitale Schmelzdefecte; Erosionen). *Dt Mschr Zahnheilk* **13**, 425–439, 483–498, 533–548, 587–600.

Boyde A (1967) The development of enamel structure. *Proc Roy Soc Med* **60**, 923–928.

Boyde A (1970) The surface of the enamel in human hypoplastic teeth. *Arch Oral Biol* **15**, 897–898.

Boyde A (1989) Enamel. In *Handbook of Microscopic Anatomy VI6 Teeth* (eds Oksche A, Vollrath L), pp. 309–473. Heidelberg: Springer.

Boyde A (1997) Microstructure of enamel. In *Dental Enamel*. *Ciba Foundation Symposium 205* (eds Chadwick D, Cardew G), pp. 18–31. Chichester: Wiley.

Brook AH, Fearne JM, Smith JM (1997) Environmental causes of enamel defects. In *Dental Enamel*. *Ciba Foundation Symposium 205* (eds Chadwick D, Cardew G), pp. 212–225. Chichester: Wiley.

Caple C (ed.) (2002) *Dryslwyn Castle excavations 1980–95: A Welsh Lord's castle of the 13th century – Excavation report*. Unpublished archive report.

Commission on Oral Health Research and Epidemiology (1982) An epidemiological index of developmental defects of dental enamel (DDE Index). *Int Dent J* **32**, 159–167.

Condon K, Rose J (1992) Intertooth and intratooth variability in the occurrence of developmental enamel defects. *J. Paleopathol Monogr Publ* **2**, 61–77.

Dean MC, Wood BA (1981) Developing pongid dentition and its use for ageing individual crania in comparative cross-sectional growth studies. *Folia Primatol* **36**, 111–127.

Diekwisch TGH (2001) The developmental biology of cementum. *Int J Dev Biol* **45**, 695–706.

Dobney K, Ervynck A (1998) A protocol for recording linear enamel hypoplasia on archaeological pig teeth. *Int J Osteoarchaeol* **8**, 263–273.

Dobney K, Ervynck A (2000) Interpreting developmental stress in archaeological pigs: the chronology of linear enamel hypoplasia. *J Archaeol Sci* **27**, 597–607.

Dobney K, Ervynck A, La Ferla B (2002) Assessment and further development of the recording and interpretation of linear enamel hypoplasia in archaeological pig populations. *Environ Archaeol* **7**, 35–46.

Dobney K, Ervynck A, Albarella U, Rowley-Conwy P (2004) The chronology and frequency of a stress marker (linear enamel hypoplasia) in recent and archaeological populations of *Sus scrofa* in north-west Europe, and the effects of early domestication. *J Zool Lond* **264**, 197–208.

Ervynck A, Dobney K (1999) Lining up on the M_1: a tooth defect as a bio-indicator for environment and husbandry in ancient pigs. *Environ Archaeol* **4**, 1–8.

Ervynck A, Dobney K (2002) A pig for all seasons? Approaches to the assessment of second farrowing in archaeological pig populations. *Archaeofauna* **11**, 7–22.

Ervynck A, Dobney K, Hongo H, Meadow R (2002) Born free? New evidence for the status of *Sus scrofa* at Neolithic Çayönü Tepesi (Southeastern Anatolia, Turkey). *Paléorient* **27**, 47–73.

Fejerskov O, Thylstrup A, Larsen MJ (1977) Clinical and structural features and possible pathogenic mechanisms of dental fluorosis. *Scand J Dent Res* **85**, 510–534.

Fejerskov O, Larsen MJ, Richards A, Baelum V (1994) Dental tissue effects of fluoride. *Adv Dent Res* **8**, 15–31.

Fejerskov O, Richards A, Den Besten P (1996) The effect of fluoride on tooth mineralization. In *Fluoride in Dentistry* (eds Fejerskov O, Ekstrand J, Burt BA), pp. 112–152. Copenhagen: Munksgaard.

FitzGerald CM, Saunders SR (2005) Test of histological methods of determining chronology of accentuated striae in deciduous teeth. *Am J Phys Anthropol* **127**, 277–290.

Franz-Odendaal TA, Lee-Thorp J, Chinsamy A (2003) Insights from stable light isotopes on enamel defects and weaning in Pliocene herbivores. *J Biosci* **28**, 765–773.

Franz-Odendaal TA (2004) Enamel hypoplasia provides insights into early systemic stress in wild and captive giraffes (*Giraffa camelopardalis*). *J Zool Lond* **263**, 197–206.

Franz-Odendaal TA, Chinsamy A, Lee-Thorp J (2004) High prevalence of enamel hypoplasia in an early Pliocene giraffid (*Sivatherium hendeyi*) from South Africa. *J Vert Paleontol* **24**, 235–244.

Goodman AH, Rose J (1990) Assessment of systemic physiological perturbations from dental enamel hypoplasias and associated histological structures. *Yrbk Phys Anthropol* **33**, 59–110.

Gustafson G, Gustafson AG (1967) Microanatomy and histochemistry of enamel. In *Structural and Chemical Organization of Teeth* (ed. Miles AEW), pp. 76–134. New York: Academic Press.

Hannibal DL, Guatelli-Steinberg D (2005) Linear enamel hypoplasia in the great apes: analysis by genus and locality. *Am J Phys Anthropol* **127**, 13–25.

Hillson S (1996) *Dental Anthropology*. Cambridge: Cambridge University Press.

Hillson S, Bond S (1997) Relationship of enamel hypoplasia to the pattern of tooth crown growth: a discussion. *Am J Phys Anthropol* **104**, 89–103.

Hillson S (2005) *Teeth*, 2nd edn. Cambridge: Cambridge University Press.

Jones SJ, Boyde A (1974) Coronal cementogenesis in the horse. *Arch Oral Biol* **19**, 605–614.

Kierdorf H, Kierdorf U (1997) Disturbances of the secretory stage of amelogenesis in fluorosed deer teeth: a scanning electron-microscopic study. *Cell Tissue Res* **289**, 125–135.

Kierdorf H, Kierdorf U, Richards A, Sedlacek F (2000) Disturbed enamel formation in wild boars (*Sus scrofa* L.) from fluoride polluted areas in Central Europe. *Anat Rec* **259**, 12–24.

Kierdorf H, Kierdorf U, Richards A, Josephsen K (2004) Fluoride-induced alterations of enamel structure: an experimental study in the miniature pig. *Anat Embryol* **207**, 463–474.

Kierdorf H, Kierdorf U, Witzel C (2005) Deposition of cellular cementum onto hypoplastic enamel of fluorotic teeth in wild boars (*Sus scrofa* L.). *Anat Embryol* **209**, 281–286.

Kierdorf U, Kierdorf H, Fejerskov O (1993) Fluoride-induced developmental changes in enamel and dentine of European roe deer (*Capreolus capreolus* L.) as a result of environmental pollution. *Arch Oral Biol* **38**, 1071–1081.

Kierdorf U, Kierdorf H, Sedlacek F, Fejerskov O (1996) Structural changes in fluorosed dental enamel of red deer (*Cervus elaphus* L.) from a region with severe environmental pollution by fluorides. *J Anat* **188**, 183–195.

Kodaka T, Kuroiwa M, Higashi S (1991) Structural and distribution patterns of surface 'prismless' enamel in human permanent teeth. *Caries Res* **25**, 7–20.

Kodaka T, Mori R, Takiguchi R, Higashi S (1995) The structural patterns and mineralisation values of prismless enamel, a case of mild enamel hypoplasia. *Bull Tokyo Dent Coll* **36**, 33–42.

Larsen CS (1997) *Bioarchaeology*. Cambridge: Cambridge University Press.

Mead AJ (1999) Enamel hypoplasia in Miocene rhinoceroses (*Teleoceras*) from Nebraska: evidence of severe physiological stress. *J Vert Paleontol* **19**, 391–397.

Mellanby M (1929) *Diet and the Teeth: an Experimental Study. Part 1, Dental Structure in Dogs*. Medical Research Council. Special Report Series no. 140. London: His Majesty's Stationery Office.

Mellanby M (1930) *Diet and the Teeth: an Experimental Study. Part 2, Diet and Dental Structure in Mammals Other Than the Dog*. Medical Research Council. Special Report Series no. 153. London: His Majesty's Stationery Office.

Mellanby M (1934) *Diet and the Teeth: an Experimental Study. Part 3, the Effect of Diet on Dental Structure and Disease in Man*. Medical Research Council. Special Report Series no. 191. London: His Majesty's Stationery Office.

Monsour PA, Harbrow DJ, Warshawsky H (1989) Effects of acute doses of sodium fluoride on the morphology and the detectable calcium associated with secretory ameloblasts in rat incisors. *J Histochem Cytochem* **37**, 463–471.

Nanci A (2003) Enamel: composition, formation and structure. In *Ten Cate's Oral Histology*, 6th edn (ed. Nanci A), pp. 145–191. St. Louis: Mosby.

Niven LB, Egeland CP, Todd LC (2004) An inter-site comparison of enamel hypoplasia in bison: implications for paleoecology and modeling Late Plains Archaic subsistence. *J Archaeol Sci* **31**, 1783–1794.

Psoter WJ, Reid BC, Katz RV (2005) Malnutrition and dental caries: a review of the literature. *Caries Res* **39**, 441–447.

Radlanski RJ (1998) Micromorphological features of human dental enamel. In *Dental Anthropology; Fundamentals, Limits, and Prospects* (eds Alt KW, Rösing FW, Teschler-Nicola M), pp. 129–145. Wien: Springer.

Risnes S (1990) Structural characteristics of staircase-type Retzius lines in human dental enamel analyzed by scanning electron microscopy. *Anat Rec* **226**, 135–146.

Risnes S (1998) Growth tracks in dental enamel. *J Hum Evol* **35**, 331–350.

Rose JC (1977) Defective enamel histology of prehistoric teeth from Illinois. *Am J Phys Anthropol* **46**, 439–446.

Sasaki T, Takagi M, Yanagisawa T (1997) Structure and function of secretory ameloblasts in enamel formation. In *Dental Enamel. Ciba Foundation Symposium 205* (eds Chadwick D, Cardew G), pp. 32–50. Chichester: Wiley.

Schroeder HE (1991) *Pathobiologie oraler Strukturen: Zähne, Pulpa, Parodont*, 2nd edn. Basel: Karger.

Smith CE (1998) Cellular and chemical events during enamel maturation. *Crit Rev Oral Biol Med* **9**, 128–161.

Smith TM (2006) Experimental determination of the periodicity of incremental features in enamel. *J Anat* **208**, 99–113.

Suckling G, Elliott DC, Thurley DC (1983) The production of developmental defects of enamel in the incisor teeth of penned sheep resulting from induced parasitism. *Arch Oral Biol* **28**, 393–399.

Suckling G, Thurley DC (1984) Histological, macroscopic and microhardness observations of fluoride-induced changes in the enamel organ and enamel of sheep incisor teeth. *Arch Oral Biol* **29**, 165–177.

Suckling G, Elliott DC, Thurley DC (1986) The macroscopic appearance and associated histological changes in the enamel organ of hypoplastic lesions of sheep incisor teeth resulting from induced parasitism. *Arch Oral Biol* **31**, 427–439.

Suckling G, Thurley DC, Nelson DGA (1988) The macroscopic and scanning electron-microscopic appearance and microhardness of the enamel, and the related histological changes in the enamel organ of erupting sheep incisors resulting from a prolonged low daily dose of fluoride. *Arch Oral Biol* **33**, 361–373.

Suckling GW, Nelson DGA, Patel MJ (1989) Macroscopic and scanning electron microscopic appearance and hardness values of developmental defects in human permanent tooth enamel. *Adv Dent Res* **3**, 219–233.

Suga S (1992) Hypoplasia and hypomineralisation of tooth enamel. *J Paleopathol Monogr Publ* **2**, 269–292.

Walton RE, Eisenmann DR (1974) Ultrastructural examination of various stages of amelogenesis in the rat following parenteral fluoride administration. *Arch Oral Biol* **19**, 171–182.

Warshawsky H, Vugman I (1977) A comparison of the protein synthetic activity of presecretory and secretory ameloblasts in rat incisors. *Anat Rec* **188**, 143–172.

Warshawsky H, Josephsen K, Thylstrup A, Fejerskov O (1981) The development of enamel structure in rat incisors as compared to the teeth of monkey and man. *Anat Rec* **200**, 371–399.

Warshawsky H (1988) The teeth. In *Cell and Tissue Biology* (ed. Weiss L), pp. 596–640. Baltimore: Urban and Schwarzenberg.

Wöltgens JHM, Lyaruu DM, Bronckers ALJJ, Bervoets TJM, Van Duin M (1995) Biomineralization during early stages of the developing tooth *in vitro* with special reference to secretory stage of amelogenesis. *Int J Dev Biol* **39**, 203–212.

Wright LE (1990) Stresses of conquest: a study of Wilson bands and enamel hypoplasias in the Maya of Lamanai, Belize. *Am J Hum Biol* **2**, 25–35.